Stringency of water conservation determines drinking water quality trade-offs: lessons learned from a full-scale water distribution system

Fatemeh Hatam[1], Gabrielle Ebacher[2], Michèle Prévost[3]

[1]NSERC Industrial Chair in Drinking Water, Dept. of Civil, Geological and Mining Engineering, Polytechnique Montréal, CP 6079, Succ. Centre-ville, Montréal, QC, Canada H3C 3A7 (corresponding author)
[2]Mechanical and Process Engineer, Water Management Service, Drinking Water Div., Laval, QC, Canada H7V 3Z4
[3]NSERC Industrial Chair in Drinking Water, Dept. of Civil, Geological and Mining Engineering, Polytechnique Montréal, CP 6079, Succ. Centre-ville, Montréal, QC, Canada H3C 3A7

A. Daily demand patterns and water quality analysis

The applied daily patterns for residential, industrial, commercial, institutional, municipal and leakage demands are shown in Figure S1.

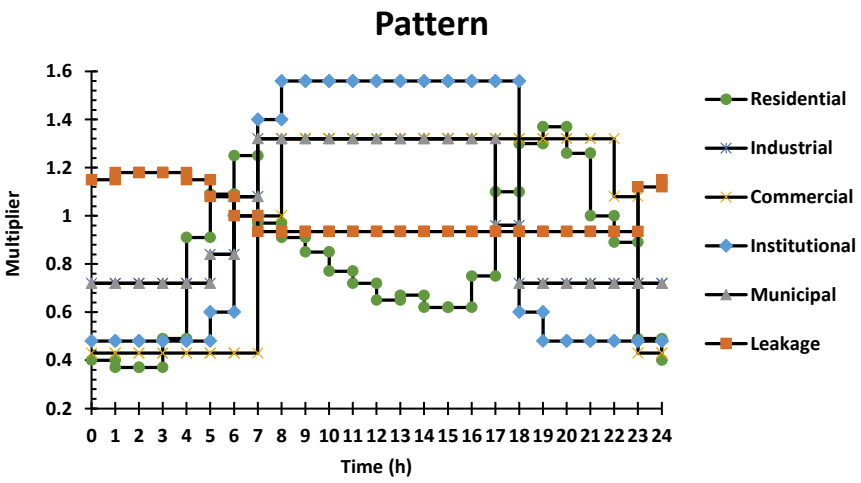

Figure S1. Daily demand patterns for different type of users.

To model chlorine, first order equations ($\frac{dC}{dt} = -KC$) for both bulk and wall decay are assumed. A mass-transfer coefficient is applied to estimate the wall consumption (Rossman, 2000):

$$K = K_b + \frac{4K_wK_f}{D(K_w + K_f)}$$

D is the pipe diameter, K_f is the mass transfer coefficient, K_b is the bulk decay constant, K_w is the wall decay constant. In this study, K_b is considered to be 1.01 day^{-1} based on experiments conducted on the studied network water (at a water temperature of 22°C and an initial chlorine concentration of 2 mg/L). K_w is selected to be 0.04 m/day based on the range of values reported in the literature (Courtis et al., 2009; Monteiro et al., 2014). THM formation is simulated considering only chlorine demand in the bulk flow, THM=K_{tc}*_Free Chlorine Bulk Consumption_, where the constant K_{tc} is considered to be 41 µg THM produced per mg of free chlorine consumed based on literature data (Boccelli et al., 2003; Courtis et al., 2009).

B. Water conservation scenarios

Table 1 describes nine water demand scenarios in which the coefficients of each scenario show reductions or increases of demand categories as compared to the current reference scenario. Different coefficients for demand variation are assigned to nodal demands according to the demand management strategy outlined in each scenario and the user types allocated to each node: residential, industrial-commercial-institutional (ICI), and municipal.

The average indoor demand used in Sc2 (221.8 LCD) is based on data from nine utilities (737 homes) across the United States and Canada (REU2016) (Water Research Foundation (WRF), 2016) . Based on all 2010 study sites, i.e. 23,749 single-family homes, 27% of the average annual water volume supplied was consumed for seasonal purposes (Water Research Foundation (WRF), 2016). It should be noted that different factors could affect outdoor usage such as homes age and weather conditions. Since this information was not available for the studied network and considering that the seasonal uses generally consists of outdoor uses, the outdoor demand in Sc2 is defined as 27% of the total residential use. To determine the residential demand of Sc3, which is considered as a past scenario, the total 2005 average day flow rate (247,400 m^3/day) is applied. This value is estimated to include 347 LCD, assuming that the only cause of demand variation compared to the 2015 average day is the residential consumption.

The current water demand scenario of Netherlands with a showering frequency of 0.7 day^{-1}, as proposed by Agudelo-Vera et al. (2016), is considered as one of the future scenarios in our study (Sc4). The residential demand consumption per person per day for the current scenario (Sc1) of the studied network located in Canada is 36% higher compared with the residential demand consumption of the actual scenario in Netherlands, from Agudelo-Vera et al. (2016). The performance of the studied network under extreme water demand variations is tested in Sc5, using the data corresponding to one of the most extreme future water conservation scenarios of residential demand in Netherlands (Eco+) (Agudelo-Vera et al., 2016). The latter scenario assumes global adoption of efficient devices and appliances including showers, dishwashers and washing machines as well as innovative sanitation concepts (Agudelo-Vera et al., 2016). In Sc6, the indoor demand is considered 139 LCD, which is associated with high efficiency fixtures and appliances according to EPA's WaterSense New Home Specifications (Aquacraft Inc. Water Engineering and Management, 2011; Water Research Foundation (WRF), 2016). The outdoor demand is set to be 27% of the total residential, as in Sc2.

In scenarios two to six, the residential demand is the only user type that has been changed as compared with the current situation. However, in scenarios seven and eight, the industrial-commercial-institutional (ICI) and municipal demands are also reduced as compared to the current scenario (Sc1). Reductions of 20% are defined based on experts' expectations when volume pricing climbs. The residential consumptions in Sc7 and Sc8 are the same as in Sc5 and Sc6, respectively. The last water conservation scenario (Sc9) investigates the impact of cutting off the industrial, commercial and institutional demands for a period of 10 days, while other demand types remain unchanged. This scenario attempts to model the impact of the extensive lockdown of industrial, commercial and institutional facilities, which can result from extreme climate events or a response to a pandemic such as the current Covid19 pandemic. The population is considered unchanged in all scenarios. The number of people supplied per node is estimated according to the nodal residential demand and the daily per capita average demand (259 L/person/day) in Sc1. The leakage demand is assumed to remain unchanged

between scenarios regardless of the impact of demand variations on pressure. However, to investigate the impact of this assumption, differential nodal water losses and nodal pressures are compared between Sc1-Sc6 and Sc1-Sc7. Based on field data, a chlorine residual of 1 mg/L is assumed at the outlet of each of the three WTPs for Sc1 to Sc9. To investigate the robustness of the studied network, the outlet chlorine concentration at each of the WTPs is increased from 1 mg/L to 2 mg/L in Sc1, Sc6 and Sc7 and are referred to Sc1B, Sc6B, and Sc7B, respectively.

C. Water loss

C.1. Methodology

Background Leakage (q_{i-leak}) for each node (i), which is a function of the leakage flows of all the pipes (k) that are connected to this node is estimated as follows (Giustolisi et al., 2008):

$$q_{i-leak} = \frac{1}{2}\sum_{k\in i} \beta_k l_k {P_k}^{\alpha_k} \qquad \text{Eq. S1}$$

where l is the length of pipe k, β and α are parameters of the leakage model, and P is the pressure. For pressure, the nodal average daily value is applied in this study; therefore, the calculated q_{i-leak} is representing the nodal average daily water loss. The exponent α can be varied between 0.5 to 2 depending on the pipe material (Berardi et al., 2015). For background leakage, α around 1.5 is suggested regardless of the pipe material (Lambert, 2001). In this study, α is considered equal to 1.5 and β is adjusted for the network through a trial-and-error process, assuming background leakage as the only source of water loss in this study. This is done by forcing the sum of all nodal average daily water losses, estimated by the above equation, to equal the total daily average leakage flow rate of the calibrated model. To calibrate β, the daily average nodal pressures are taken from the current scenario (Sc1).

C.2. Results

The distribution of pressure differences and the percentage of difference in nodal water loss due to changes in water demand are compared for two of the water conservation

scenarios in relation to the current scenario (Figure S2). The median percentage of nodal water loss difference between Sc1 and Sc6 is 2% and between Sc1 and Sc7 is 4% (Figure S2, b), while the maximum values reach to 19% and 26%, respectively. These differences come from the pressure variations due to changes in water demand (Figure S2, a). Using the daily average nodal pressures (Eq. S1), the estimated amount of average daily water losses for the whole network in Sc1, Sc6 and Sc7 would be 609, 629, and 643 L/s, respectively. These results indicate an increase of 3% for Sc6 and 6% for Sc7 as compared to the current scenario (Sc1), in line with the reported value by Zhuang and Sela (2020) who observed a 6% increase in water loss in the case of 50% reduction of the residential demand. In our study, the leakage demand was kept unchanged, regardless of the pressure variations under different demand scenarios. However, in future studies, this impact could be included in the model by implementing a more realistic leakage model based on nodal pressure variations calculated through a pressure-driven equation as in Kabaasha et al. (2018). In fact, the outlet pressure at the three WTPs should be adjusted based on the outflow from the plant and on pressure measurements from strategic network monitoring sites in order to reduce pressure fluctuations in the network under various demand conditions. Depending on the demand management program, which defines the severity and spatial distribution of demand reduction in the network, decreasing the pressure at the pumping system or implementing district-metered areas with pressure regulation are actions aimed at maintaining the robustness of the network by preventing major increases in water loss.

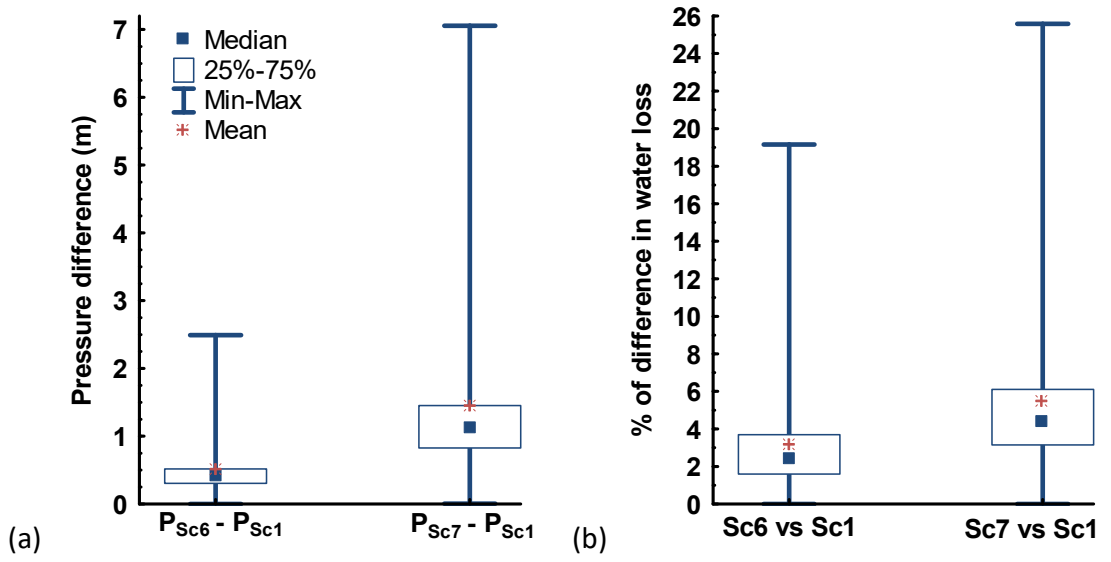

Figure S2. Box-plot showing (a) nodal pressure differences between two scenarios Sc6-Sc1 and Sc7-Sc1, and (b) the percentage of difference in nodal water loss of Sc6 and Sc7 compared to Sc1.

D. Impact of demand variations on water age

Figure S3 compares distributions of nodal water age of Sc1 to Sc8 for four groups of nodes categorized based on the largest diameter of the pipe connected to that node. Higher water age values occur mainly at pipes with a smaller diameter. The median water age values decrease within the range of 3-4 h under various demand scenarios for the nodes that are connected to pipes with D>800 mm (associated pipe length = 21 km). In the current scenario (Sc1), 13% of nodes have maximum water age more than 30 h, while this value increases to 36% in Sc7, which is the most water conservative scenario. In the studied network, 67% of the pipe length consists of 200 mm diameter pipes or smaller, while only about 1% of the pipe length has a diameter larger than 800 mm.

Since the studied network provides water to both residential and non-residential users, the network performance is also assessed by reducing the industrial-commercial-institutional (ICI) demand by 20% in Sc7 and Sc8. Figure S3 shows that the same decrease in ICI demand resulted in slightly different changes in median water age under different factors of residential demand reductions. For small pipes (D≤200 mm), the median water age is increased by 1.5 hours (Sc7) and 0.7 hours (Sc8) as compared with Sc5 and Sc6, in

which residential demands are reduced by a multiplicative factor of 0.18 and 0.73, respectively. The residential consumptions in Sc7 and Sc8 are the same as in Sc5 and Sc6, respectively. While considering only the effect of residential demand reduction in Sc5 and Sc6, an increase of 7.6 h and 1.5 h in median water age is observed for small pipes (D≤200 mm) as compared to the current scenario (Sc1) (Figure S3).

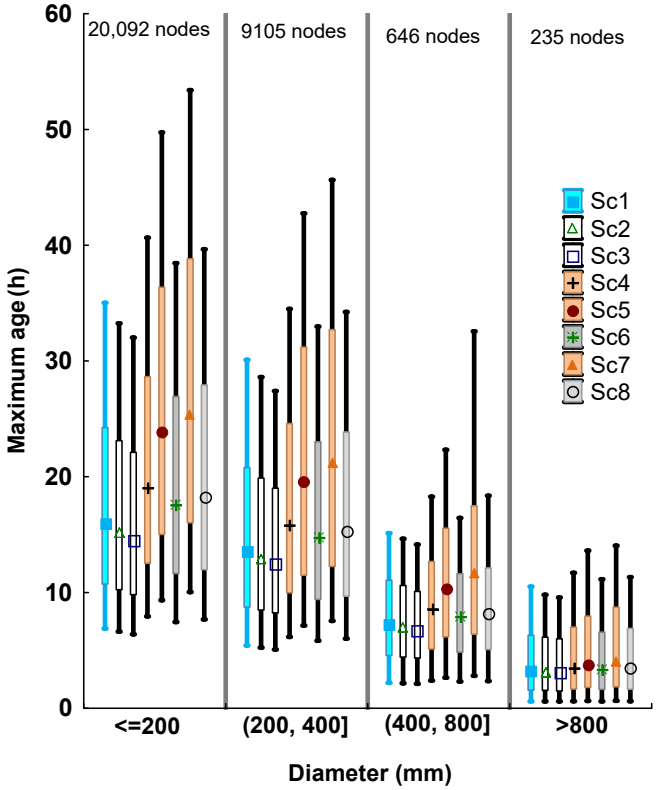

Figure S3. Distribution of nodal water age for scenarios 1 to 8 for four groups of nodes. Nodes are categorized based on the largest pipe diameter connected to them. Median; Box: 25%-75%; Whisker: 10%-90%.

E. Impact of demand variations on chlorine residuals

Figure S4 shows number of nodes for various ranges of minimum chlorine residual in Sc1, Sc3, Sc6, and Sc7. It is shown that in Sc1, Sc3, and Sc6 more than 80% of the nodes had chlorine residual more than 0.2 mg/L all over the day, while this value is about 60% in Sc7.

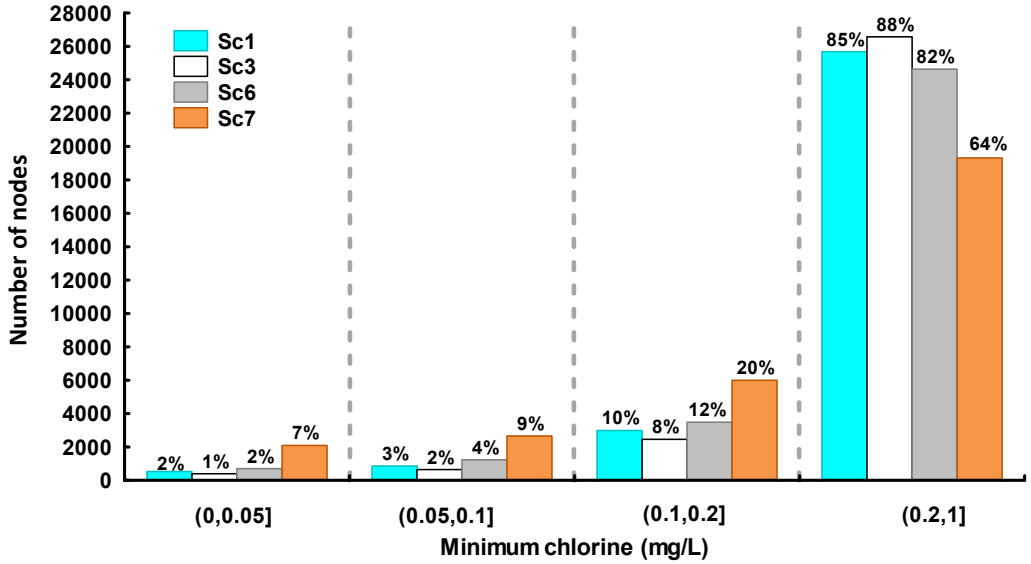

Figure S4. Number of nodes for various ranges of minimum chlorine residuals (Cl2≤0.05, 0.05<Cl2≤0.1, 0.1<Cl2≤0.2, 0.2<Cl2≤0.5, Cl2>0.5 mg/L) in Sc1, Sc3, Sc6, and Sc7.

F. Varaitions of nodal chlorine residuals and THMs during the day

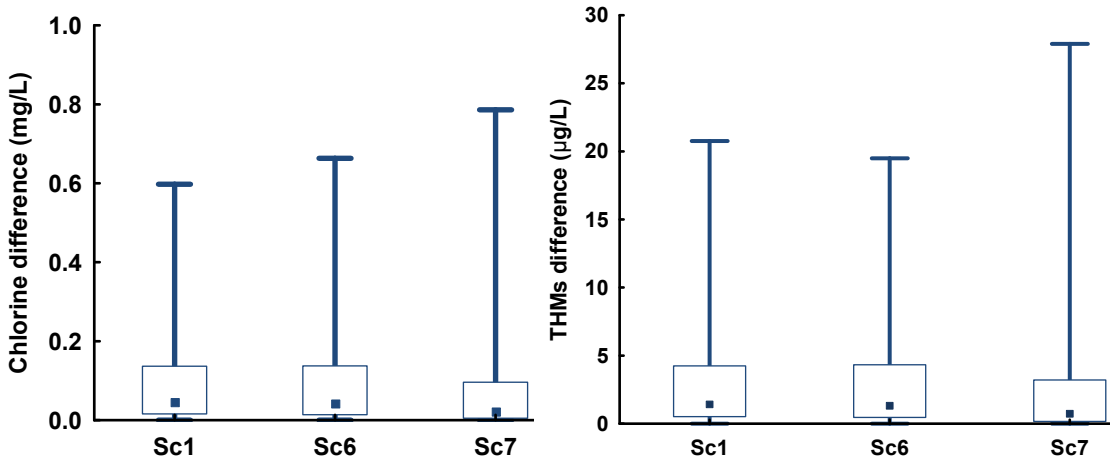

Figure S5. Distribution of chlorine residuals and THMs nodal differences between maximum and minimum values during the day in Sc1, Sc6 and Sc7. Median; Box: 10%-90%; Whisker: Min-Max.

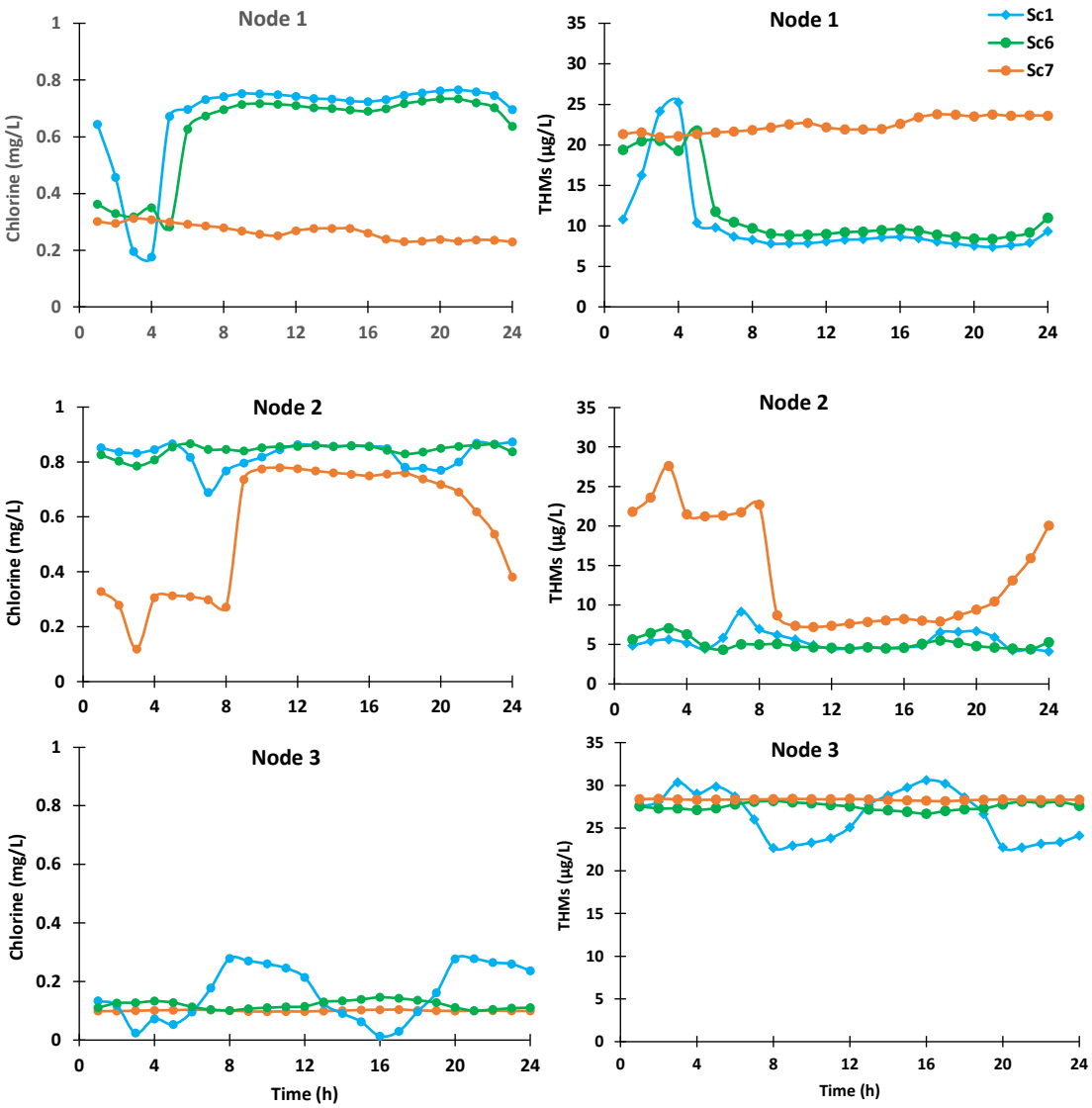

Figure S6. Examples of variations of chlorine residuals and associated THM values during the day for 3 nodes of the studied network

G. Pipe velocity

Pipe length with V_{max}≥0.2 m/s and D≤200 mm for scenarios of average day (ScA), average winter day (ScB) and maximum day (ScC) is shown in Table S1.

Table S1. Fraction of pipe length with self-cleaning capacity for scenarios of average day (ScA), average winter day (ScB) and maximum day (ScC) (Table 1). Total pipe length is 1628 km and 67% of pipe length consists of 200 mm or smaller diameter pipes

Scenarios	ScA	ScB	ScC
Pipe length (km) with V_{max}≥0.2 m/s and D≤200 mm	51	42	160
Percentage of length considering only D≤200 mm	5%	4%	15%

Figure S7 shows maximum daily velocity versus pipe diameter for scenarios of average day, average day winter and maximum day.

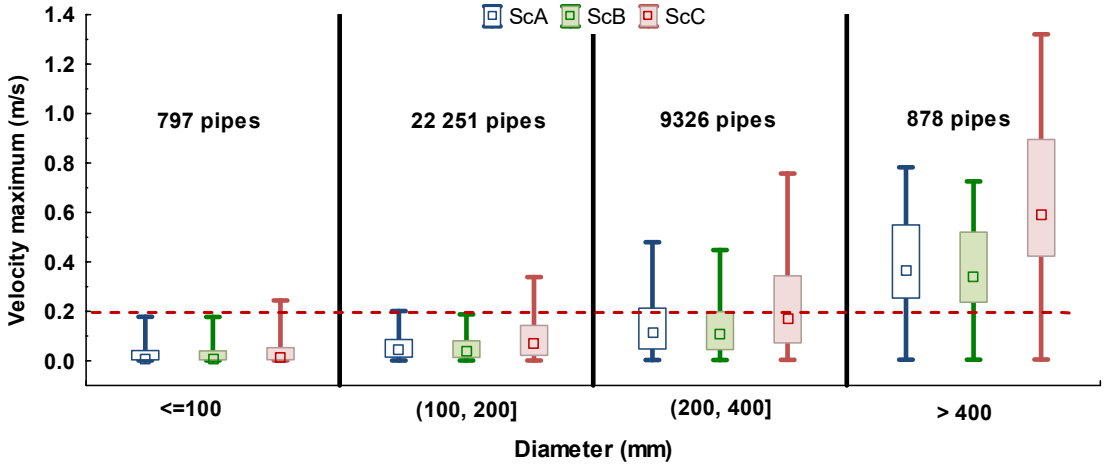

Figure S7. Maximum velocity versus pipe diameter for scenarios A, B and C. Median; Box: 25%-75%; Whisker: 5%-95%.

H. References

Agudelo-Vera, C., Blokker, M., Vreeburg, J., Vogelaar, H., Hillegers, S., van der Hoek Jan, P. (2016) Testing the robustness of two water distribution system layouts under changing drinking water demand. Journal of Water Resources Planning and Management 142, 05016003.

Aquacraft Inc. Water Engineering and Management, (2011) Analysis of water use in new single-family homes. Submitted to Salt Lake City Corporation and USEPA, in: DeOreo, W.B. (Ed.), p. 156.

Berardi, L., Laucelli, D., Ugarelli, R., Giustolisi, O. (2015) Hydraulic system modelling: Background leakage model calibration in oppegård municipality. Procedia Engineering 119, 633-642.

Boccelli, D.L., Tryby, M.E., Uber, J.G., Summers, R.S. (2003) A reactive species model for chlorine decay and THM formation under rechlorination conditions. Water Research 37, 2654-2666.

Courtis, B.J., West, J.R., Bridgeman, J. (2009) Chlorine demand-based predictive modeling of THM formation in water distribution networks. Urban Water Journal 6, 407-415.

Giustolisi, O., Savic, D., Kapelan, Z. (2008) Pressure driven demand and leakage simulation for water distribution networks. Journal of Hydraulic Engineering 134, 626-635.
Kabaasha, A.M., Piller, O., van Zyl, J.E. (2018) Incorporating the modified orifice equation into pipe network solvers for more realistic leakage modeling. Journal of Hydraulic Engineering 144.
Lambert, A., (2001) What do we know about pressure: Leakage relationships in distribution systems?, IWA System Approach to Leakage Control and Water Distribution Systems Management, Brno, Czech Republic, p. 8.
Monteiro, L., Figueiredo, D., Dias, S., Freitas, R., Covas, D., Menaia, J., Coelho, S.T. (2014) Modeling of chlorine decay in drinking water supply systems using EPANET MSX. Procedia Engineering 70, 1192-1200.
Rossman, L.A., (2000) EPANET 2. User's manual. National Risk Management Research Laboratory, Office of Research and Development, United States Environmental Protection Agency (USEPA), Cincinnati, Ohio, USA, p. 200.
Water Research Foundation (WRF), (2016) Residential end uses of water, version 2, p. 363.
Zhuang, J., Sela, L. (2020) Impact of emerging water savings scenarios on performance of urban water networks. Journal of Water Resources Planning and Management 146, 04019063.